



CrossMark
click for updates

Cite this: *React. Chem. Eng.*, 2017, 2, 68

A general [¹⁸F]AlF radiochemistry procedure on two automated synthesis platforms†

L. Allott,‡ C. Da Pieve,‡ D. R. Turton and G. Smith*

The aluminium fluoride-18 ([¹⁸F]AlF) radiolabelling procedure has generated great interest because it is a simple, one-pot method that can be used to directly radiolabel small molecules, peptides and proteins without the requirement for a [¹⁸F]fluoride drying step. Reported here is the development of an automated [¹⁸F]AlF radiolabelling procedure of three different precursors (one small molecule and two peptides) on two automated synthesis platforms: GE TRACERlab FX_{FN} and Trasis AllInOne (AIO). Aiming at the clinical translatability of a [¹⁸F]AlF radiosynthetic methodology, the use of both platforms yielded radioconjugates with >98% radiochemical purity (RCP) within 26–35 min and required a single rapid purification step. The Trasis AIO platform gave improved [¹⁸F]fluoride incorporation, and generally produced radioconjugates with a higher radiochemical yield (RCY) and effective specific activities (SA) when compared to the GE TRACERlab FX_{FN} system.

Received 9th November 2016,
Accepted 16th January 2017

DOI: 10.1039/c6re00204h

rsc.li/reaction-engineering

Introduction

Positron emission tomography (PET) is an imaging modality used to diagnose and stage diseases by quantitatively monitoring the *in vivo* distribution of a positron emitting radionuclide bound by chelation or covalent bonding to a biological targeting molecule. Fluorine-18 is often considered the “ideal” PET radioisotope due to a combination of its high positron emission (97%), low positron energy ($\beta^+_{\max} = 0.64$ MeV) ensuring relatively high resolution images and its half-life (109.8 min) which is compatible with multistep synthesis and off-site transport.¹ Generally, the incorporation of fluorine-18 into small organic molecules requires high temperatures and the use of organic solvents; unfortunately these conditions are unsuitable for the labelling of biomolecules such as peptides and small proteins.² As a consequence, their radiolabelling can be achieved by a post-radiolabelling attachment of fluorine-18 containing small molecules *e.g.* *N*-succinimidyl 4-[¹⁸F]-fluorobenzoate ([¹⁸F]SFB) using mild aqueous conditions.³ Recently, investigation into the direct radiolabelling of biomolecules with fluorine-18 yielded a one-step procedure comprising the chelation of the aluminium fluoride-18 complex ([¹⁸F]AlF) by a macrocyclic ligand (*i.e.* NOTA, NODA).^{4–7}

The rapid [¹⁸F]AlF technique has generated significant interest owing to the combination of convenient metal based radiochemistry and the excellent decay characteristics of fluorine-18. This approach has been used to successfully radiolabel clickable tags, peptides and small proteins.^{5,8–12}

McBride *et al.* described the preparation of a lyophilised kit which provided a potential starting point for the standardised production of [¹⁸F]AlF-based radiopharmaceuticals.⁷ Additionally, Yu *et al.* reported the feasibility of [¹⁸F]AlF radiolabelled NOTA-PRGD2 “[¹⁸F]Alfatide” in healthy volunteers and in patients with brain metastases.¹³ This demonstrates an increased interest in applying the [¹⁸F]AlF radiolabelling technique for the preparation of radiopharmaceuticals for clinical application.

This study describes the development of a general [¹⁸F]AlF automated radiolabelling procedure. Two different platforms, a GE TRACERlab FX_{FN} and a Trasis AllInOne (AIO), were trialled and three azamacrocyclic-containing substrates were radiolabelled (Fig. 1). NOTA-octreotide and NOTA-RGDfK were selected because they are commercially available and have been previously extensively radiolabelled using the [¹⁸F]AlF method.^{14–16} The tetrazine functionalised NODA macrocycle (NODA-Tz) was used as a representative of small molecules. Compounds having a similar structure to NODA-Tz have been radiolabelled with the [¹⁸F]AlF complex and employed for the bioorthogonal pre-clinical imaging of tumour xenografts in mice.⁸ The two automated platforms used in the study are widely used for the production of radiopharmaceuticals under GMP conditions.

The GE TRACERlab FX_{FN} is built around a fixed reactor vessel with components which are attached to fixed locations.

Division of Radiotherapy and Imaging, The Institute of Cancer Research, 123 Old Brompton Road, London, SW7 3RP, UK. E-mail: graham.smith@icr.ac.uk; Fax: +44 (0)2073705261; Tel: +44 (0)2087224482

† Electronic supplementary information (ESI) available: Materials and methods, analytical data for tetrazine (¹H/¹³C NMR and MS), RP-HPLC chromatograms and GE Tracer Lab FX FN radiolabelling efficiency table. See DOI: 10.1039/c6re00204h

‡ Equal contribution for first authorship.



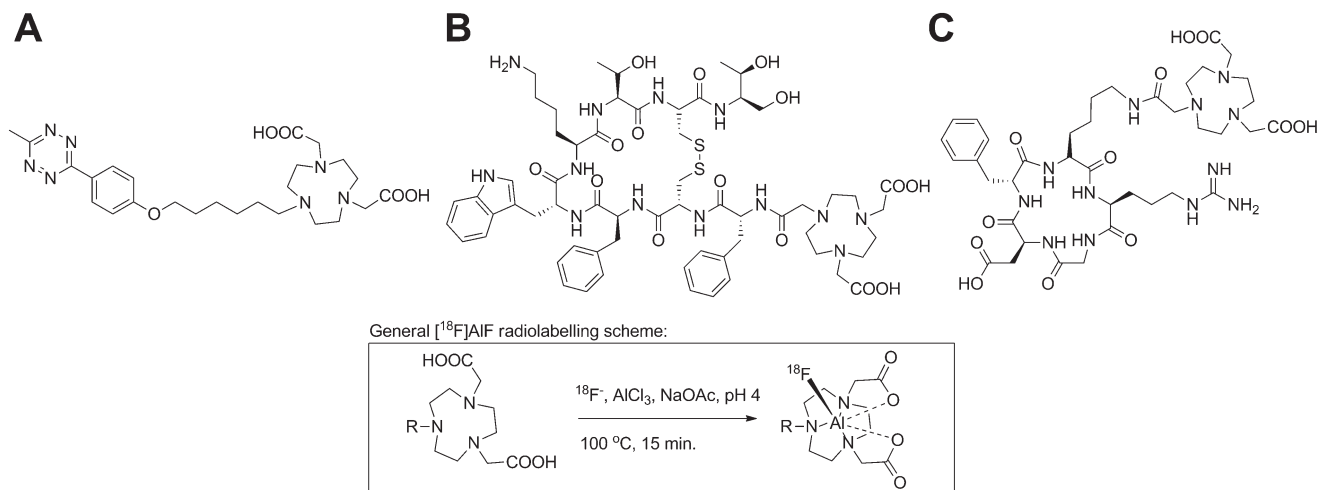


Fig. 1 The three different azamacrocycle-containing substrates used in the study: NODA-Tz (A), NOTA-octreotide (B), NOTA-RGDfK (C) and the general radiolabelling reaction (insert).

Reagents are manipulated from glass reservoirs to the reactor by gas pressure. The Trasis AIO platform is a cassette based system that mimics hands on processes (*e.g.* with the use of replaceable syringes and plastic manifolds) by using syringe drives and tap turners; as the cassette is a disposable component, the synthesis is more GMP compatible than a fixed reactor system. Additionally, the platforms are managed by two different types of automation software. In the GE TRACERlab FX_{FN} system, the process is controlled by a time list with only limited feedback from the platform. The Trasis AIO process is controlled by a combination of timed steps and feedback from the platform regarding that the correct syringe position, temperature or pressure has been achieved.

In this study, the radiolabelling was initially investigated on the GE TRACERlab FX_{FN} system to find indicative trends in radiolabelling performance by changing reaction conditions (*e.g.* volumes, buffer and substrate quantities) which were subsequently applied to the Trasis AIO platform.

Results and discussion

Selection and preparation of the substrates

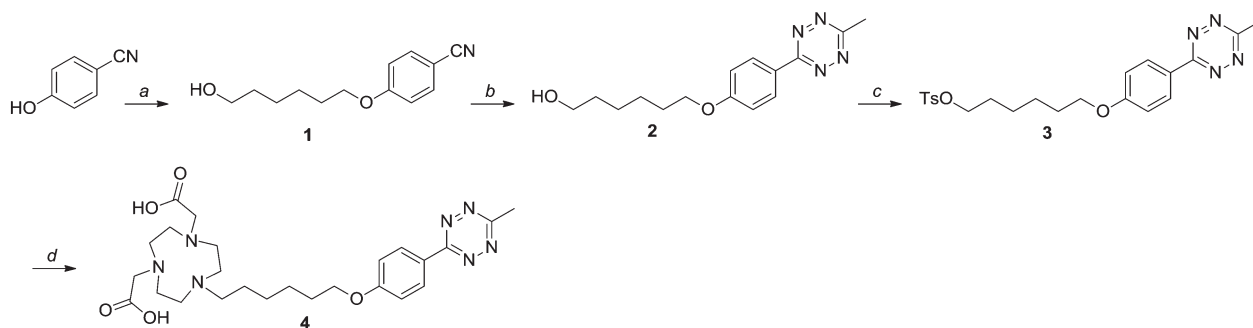
Two commercially available azamacrocycle-conjugated peptides (NOTA-octreotide and NOTA-RGDfK) and the non-

commercially available tetrazine functionalised 1,4,7-triazacyclononane-1,4-diacetic acid (NODA-Tz) were selected for this study to represent the different molecules which have been radiolabelled *via* the [¹⁸F]AlF method (Fig. 1).

The NODA-Tz small molecule (4) has been designed and synthesised in our lab (Scheme 1). Having previously shown a high [¹⁸F]AlF radiolabelling efficiency, the NODA macrocycle was chosen in preference to the more commonly used NOTA chelator.^{5,17} In brief, product 4 was prepared by attaching a 6-carbon alkyl linker to 4-cyanophenol to access compound 1 which was converted into tetrazine 2 in one step following a simple literature procedure.¹⁸ Tetrazine 3, derived from the tosylation of 2, was reacted with NO₂AtBu and subsequently deprotected using TFA. The desired product 4 was obtained in a high purity after RP-HPLC purification. All purified compounds were characterised by ¹H and ¹³C-NMR and ESI-HRMS (ESI⁺).

[¹⁸F]AlF radiolabelling conditions using GE TRACERlab FX_{FN} automated synthesis platform

Previously, [¹⁸F]AlF radiolabelling has been performed by hand using non-purified [¹⁸F]fluoride (*i.e.* not treated to remove metal residues) with an optimal reaction pH of 4 which



Scheme 1 Synthesis of NODA-Tz (4). Reaction conditions: a) 6-bromohexanol, K₂CO₃, acetone, 56 °C, 24 h; b) hydrazine hydrate, Ni(OTf)₂, MeCN, 60 °C, 16 h; c) *p*-toluenesulfonyl chloride, TEA, DCM, r.t., 16 h; d) i. NO₂AtBu, DIPEA, DMF, RT, 16 h; ii. TFA, RT, 2 h.



is usually achieved using small volumes of a concentrated buffer solution (e.g. 10 μL of 0.5 M NaOAc).⁵ The reaction mixture is then incubated at 100–105 $^{\circ}\text{C}$ for 15 min and a small excess of the macrocycle-conjugate over Al^{3+} is recommended.¹⁴ Typically, the presence of an organic co-solvent (ethanol or acetonitrile) improved the radiolabelling efficiency.¹⁵ Generally, the lowest achievable final reaction volumes (i.e. highest conjugate concentration) and acetate ion concentration afforded increased radiolabelling yields.¹⁴ Both automation systems used in this study are designed for handling large volumes of liquid and therefore the conventional [^{18}F]AlF radiolabelling conditions required modification. To improve the RCY, a glass reactor was used for the radiolabelling of peptides, while a glassy carbon reactor was used for the NODA-Tz. For an efficient transfer to the reaction vessel, the substrate was dissolved in NaOAc buffer (ca. 100 μL , 25 mM, pH 4) and a portion of the organic co-solvent (100 μL). The volume of NaOAc was carefully selected to buffer the [^{18}F]fluoride (300–380 μL aliquot, ca. 1000 MBq, of ca. 2 mL target water) to the optimal pH of 4 while minimising the effect of dilution on the radiolabelling efficiency. A conjugate to AlCl_3 molar ratio of 1:0.9 was used.

Acetonitrile was selected as the organic co-solvent for the NODA-Tz substrate due to poor solubility in ethanol. The radiolabelling of NOTA-RGDfK and NOTA-octreotide substrates using a different co-solvent (i.e. ethanol) resulted in no difference in performance (RCYs). Acetonitrile was used with all three substrates to ensure consistency of the general method. The co-solvent was used in an aqueous solution in the ratio of 1:1.2 (v/v) which was found to give the best [^{18}F]AlF incorporation without loss of efficiency due to excessive dilution (data not shown). An efficient radiolabelling, without degrading the structural integrity of the molecules, was achieved by incubating the mixture at 105 $^{\circ}\text{C}$ for 15 min. The use of ascorbic acid as a radioprotector was necessary for peptide labelling as extensive radiolysis was observed (Fig. S1, S3B and S4B[†]). A radioprotector was not required for the radiosynthesis of [^{18}F]AlF-NODA-Tz.

If larger volumes of [^{18}F]fluoride are to be used, a concentration step using an anion exchange cartridge could be employed and placed before the reactor on the GE TRACERlab FX_{FN} (Fig. 2) and eluted following the procedure described by Meyer *et al.*⁸ Alternatively, the production of a high radioactive concentration of [^{18}F]fluoride for clinical

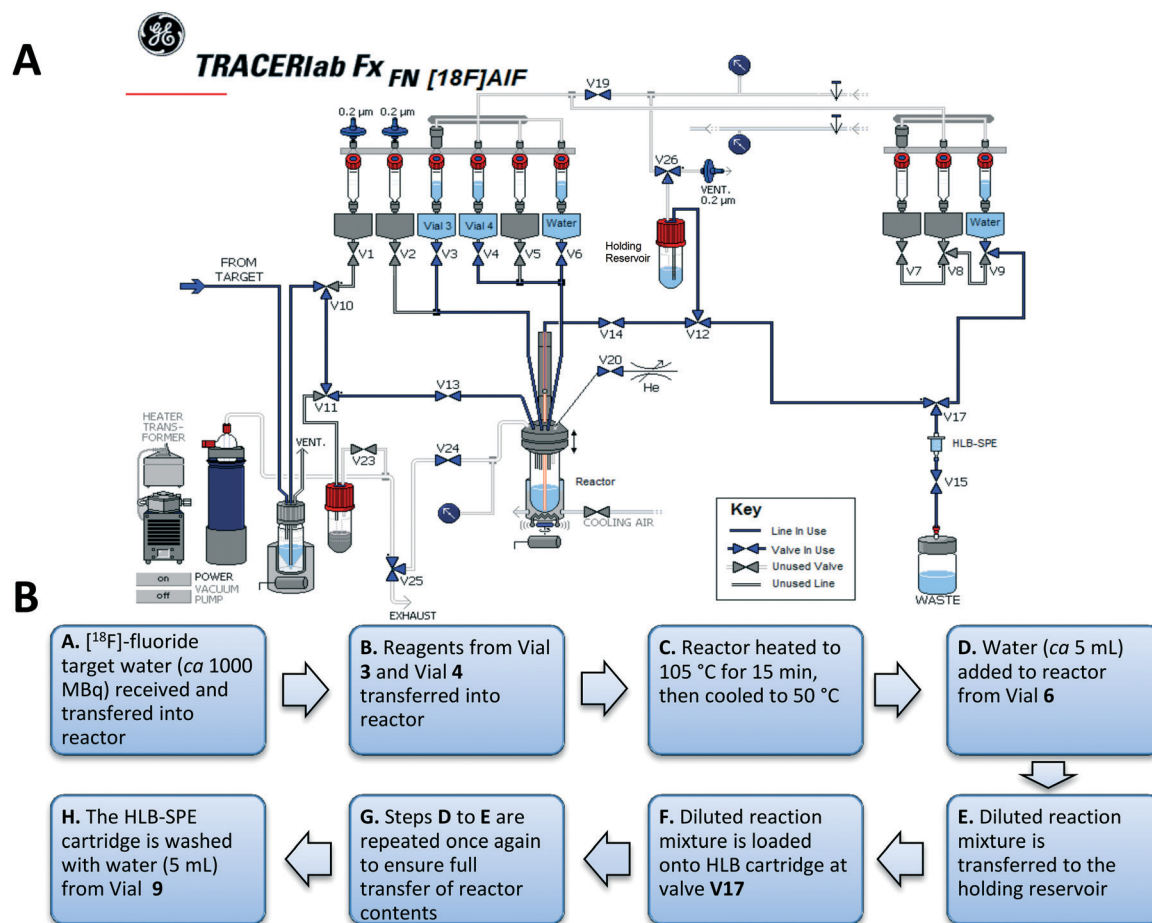


Fig. 2 Schematic representation of the [^{18}F]AlF radiochemistry set up (A) and overview of the automated radiolabelling processes (B) for the GE TRACERlab FX_{FN} system. If necessary, an anion exchange cartridge can be placed between V10 and V11 to concentrate the [^{18}F]fluoride solution followed by elution into the reaction vessel from V1.



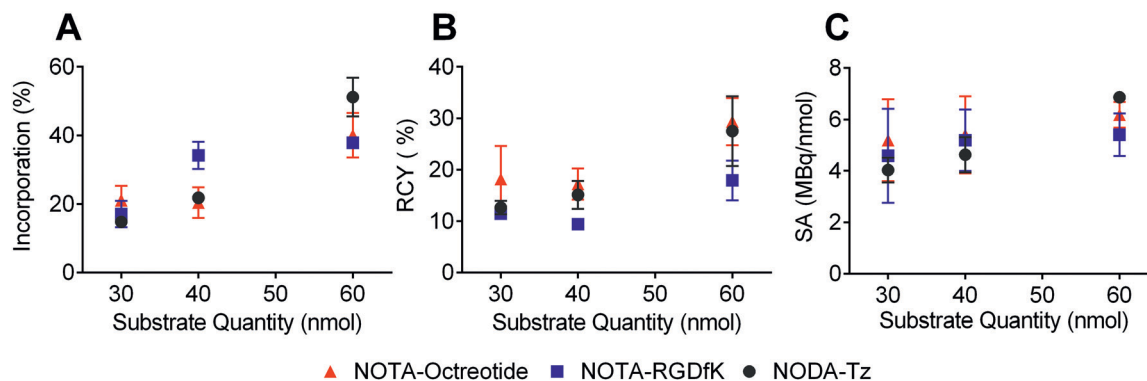


Fig. 3 Correlation between the quantity of substrate and [^{18}F]fluoride incorporation degree (A), RCY (isolated and decay corrected to the start of reaction) (B) and SA (effective specific activity) (C) using the GE TRACERlab FX_{FN} system using ca. 1000 MBq of non-purified [^{18}F]fluoride. The reactions were performed in triplicate ($n = 3$). The results are presented as mean \pm SD.

applications will remove the necessity of a [^{18}F]fluoride concentration procedure; instead, a concentrated [^{18}F]fluoride aliquot (300–380 μL) can be used directly with this method.

The effect of the conjugate amount on the incorporation, radiochemical yield (RCY, isolated and decay corrected to the start of reaction) and effective specific activity (SA) of the final radioconjugates was subsequently investigated. For this purpose three quantities of substrate (30, 40, and 60 nmol) were radiolabelled using the same amount of [^{18}F]fluoride activity (ca. 1000 MBq). The incorporation of [^{18}F]fluoride was determined from the RP-HPLC chromatogram of the crude reaction mixture, however unreacted [^{18}F]fluoride can be retained on the HPLC column which could lead to over-estimation of the incorporation.¹⁹

As shown in Fig. 3 and Table S1,[†] an increase of the quantities of each of the studied compounds corresponds to an improvement of the [^{18}F]fluoride incorporation, RCY and the SA of the final product. Mostly, the incorporation and radiochemical yields appear to increase with increased amount of conjugate. Effective specific activities of the final products are less affected by the initial substrate quantity. However, full optimisation of the [^{18}F]AlF radiolabelling was beyond the scope of this work and would be largely dependent on the local requirements of the application for the radioconjugate.

A single final purification step using HLB-SPE was sufficient to access the final radioconjugates with a RCP >98% (Fig. S2B, S3B, and S4B[†]). To ensure that the SPE cartridge was efficiently trapping the products and therefore providing the best RCY possible, a test using two cartridges placed in series was carried out. The presence of a negligible amount of radioactivity trapped on the second cartridge confirmed that the products were efficiently loaded by the automated system and were effectively trapped onto the HLB-SPE cartridge. The radioconjugates were eluted with 50% EtOH/H₂O (300–500 μL) and were suitable for use in pre-clinical applications after dilution with either PBS or 0.9% sodium chloride solution. The total production time was 35 min. A schematic representation of the GE TRACERlab FX_{FN} system is shown in Fig. 2 together with a list of the radiolabelling reaction

steps. A more detailed description of the automated radiolabelling process can be found in the ESI[†] (Materials and methods, Section 3).

Automated synthesis and formulation using the Trasis AIO platform and comparison with the GE TRACERlab FX_{FN} system

The radiosynthesis of the three [^{18}F]AlF radioconjugates was performed on the Trasis AIO platform using the best radiolabelling conditions acquired from the GE TRACERlab FX_{FN} system. In brief, 60 nmol of each conjugate was reacted with non-purified [^{18}F]fluoride (300–380 μL aliquot, ca. 1000 MBq, of ca. 2 mL target water), AlCl₃ (1:0.9 substrate to Al³⁺ molar ratio) at pH 4 (achieved using NaOAc buffer 25 mM). Acetonitrile was used as organic co-solvent (aqueous solution to organic solvent ratio of 1:1.2 v/v) and the reaction mixture was incubated at 105 °C for 15 min.

A schematic representation of the Trasis AIO system is shown in Fig. 5 together with a list of the radiolabelling reaction steps. A more detailed description of the automated radiolabelling process can be found in the ESI[†] (Materials and methods, Section 4).

The production time was 26 min. [^{18}F]AlF-NODA-Tz and [^{18}F]AlF-NOTA-octreotide showed a >60% [^{18}F]fluoride incorporation, a >45% RCY, and a >10 MBq nmol⁻¹ SA (Table 1). As seen in Fig. 4, the [^{18}F]fluoride incorporation, the RCY and SA of the radioconjugates were generally higher when the Trasis AIO platform was used compared to the GE

Table 1 Radiolabelling efficiency using the cassette based Trasis AIO platform with ca. 1000 MBq of non-purified [^{18}F]fluoride. Reactions were performed in triplicate ($n = 3$) and the results are presented as mean \pm SD. RCY (isolated and decay corrected to the start of reaction). SA (effective specific activity)

Substrate	Quantity (nmol)	Incorporation (%)	RCY (%)	SA (MBq nmol ⁻¹)
NODA-Tz	60	68.1 \pm 6.1	48.2 \pm 1.4	11.4 \pm 2.0
NOTA-RGDfK	60	48.3 \pm 10.6	15.3 \pm 6.5	7.4 \pm 1.1
NOTA-octreotide	60	75.0 \pm 1.8	56.2 \pm 4.2	12.7 \pm 0.14



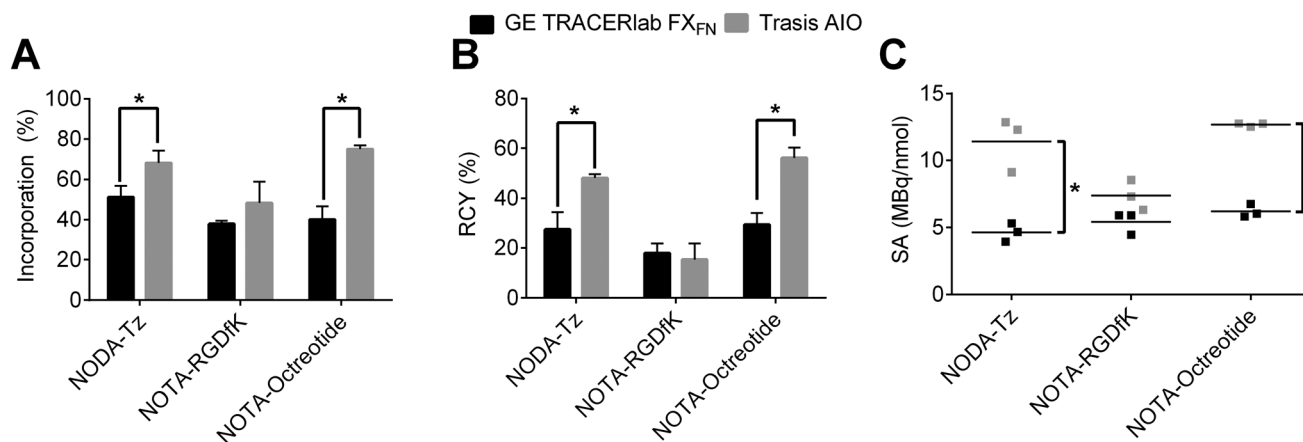


Fig. 4 Comparison of the [¹⁸F]fluoride incorporation degree (A), RCY (isolated and decay corrected to the start of reaction) (B) and SA (effective specific activity) (C) between the GE TRACERlab FX_{FN} and Trasis AIO automated synthesis platforms when 60 nmol of each precursor and a non-purified [¹⁸F]fluoride activity of ca. 1000 MBq were used. Statistical significance was determined using a paired t-test (*P < 0.05).

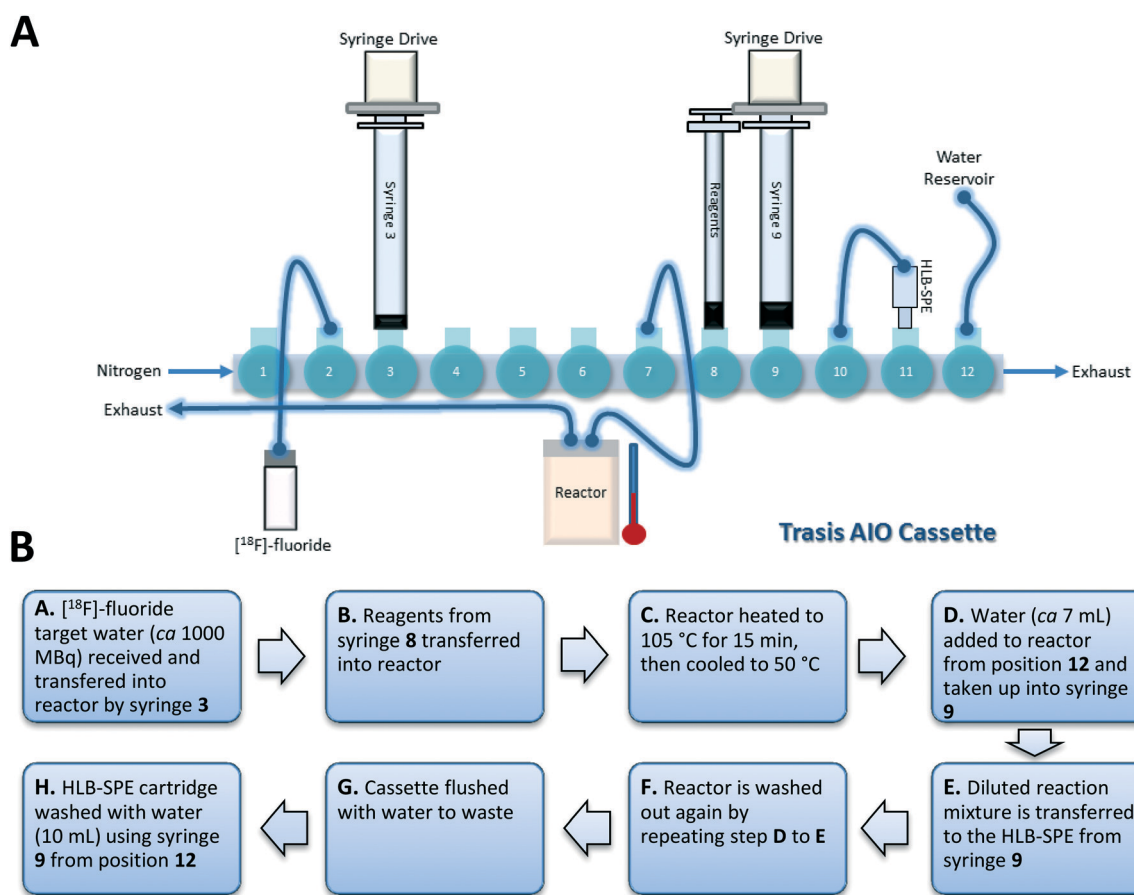


Fig. 5 Schematic representation of the [¹⁸F]AlF radiochemistry set up (A) and overview of the automated radiolabelling processes (B) for the Trasis AIO system.

TRACERlab FX_{FN} system. The effective control over the movement of reagents and reaction mixtures around the Trasis AIO cartridge based system may be responsible for that. However, the overall production efficiency of the [¹⁸F]AlF-NOTA-RGDfK radioconjugate showed minimal variation between

the two platforms. This suggests that the radiolabelling procedure and purification were dependent not only on the reaction conditions but also on the physical and structural properties of the molecules of interest (*e.g.* amino acid sequence, chain length) which could influence the interaction with the



surfaces of the reaction vessels and tubing of the automation platform.

The general radiolabelling method described here can be used as a starting point for further optimisation to progress a substrate of interest into a clinical setting.

Conclusions

Automated processes are typically required for the production of good manufacturing process (GMP) compliant fluorine-18 radiopharmaceuticals. Examples of PET imaging agents manufactured using this approach include [^{18}F]FLT, [^{18}F]FAZA, [^{18}F]HX4 and [^{18}F]ICMT-11; where the use of automated platforms has facilitated the progression of these radiotracers into the clinic.^{20–24} Automation of radiopharmaceutical production is desirable to reduce the risk to patients by enabling batch reporting/record keeping, management control and standardisation of processes through the use of standard operating practices (SOPs). Furthermore, production methods are carefully validated to ensure that processes do not introduce pyrogens, microbes or particles into the final patient dose. In addition to reducing the radiochemists contact with the final product, the automation of radiosynthesis and dispensing of the patient dose may reduce the number of batch failures resulting from human error. Automated synthesis modules, particularly cassette based systems, are ideal for use in GMP radiosynthesis as most components are easy to obtain in sterilised packaging and are disposable after a single production run, eliminating the need to further validate a post-production cleaning step. Secondly, these systems are easy to shield which addresses radiation safety concerns associated with handling large amounts of radioactivity.²⁵

This study aimed to develop a general method suitable for the automation of [^{18}F]AIF radiochemistry which was applied to the GE TRACERlab FX_{FN} and Trasis AIO platforms. The radiolabelling conditions were studied using a selection of azamacrocyclic-containing molecules including two commercially available peptides and one in-house synthesised small molecule. Initially, the [^{18}F]AIF radiochemistry was developed using the GE TRACERlab FX_{FN} system and subsequently transferred to the Trasis AIO platform. Purification of the products by HLB-SPE was sufficient to provide radioconjugates with high radiochemical purity (>98%) and the total reaction times were 26–35 min. Currently, the method described is suitable for accessing radioconjugates for pre-clinical studies. Further work would be required to maximise radiochemical yield for a chosen substrate and to optimise the purity profile of the final product prior to patient use. This process should ensure that regulatory parameters are met. The production of large radioactivity batches of GMP grade radiopharmaceuticals for multi-patient doses allows off-site transportation to “satellite” PET centres and facilitates commercial accessibility to these imaging agents. Although the final products were successfully prepared using both automated systems, the cassette based Trasis AIO en-

abled the highest [^{18}F]fluoride incorporation and gave products with the highest RCY and SA compared to the GE TRACERlab FX_{FN}, most likely due to a greater control over reagent handling. Both the GE TRACERlab FX_{FN} and Trasis AIO systems can be used for the [^{18}F]AIF radiolabelling of peptides and small molecules and have great potential for the cGMP productions of [^{18}F]AIF radiopharmaceuticals for routine clinical use.

Abbreviations

NOTA	1,4,7-Triazacyclononane-1,4,7-triacetate
NODA	1,4,7-Triazacyclononane-1,4-diacetate
TCO	<i>trans</i> -Cyclooctene
IEDDA	Inverse-electron demand Diels–Alder
NO2AtBu	2,2'-(1,4,7-Triazacyclononane-1,4-diyl)diacetate
DIPEA	<i>N,N</i> -Diisopropylethylamine
TFA	Trifluoroacetic acid
RCP	Radiochemical purity
SPE	Solid phase extraction
Rt	Retention time
NaOAc	Sodium acetate
DMSO	Dimethyl sulfoxide
DCM	Dichloromethane
EtOAc	Ethyl acetate
EtOH	Ethanol
DMF	Dimethylformamide
SA	Effective specific activity
SD	Standard deviation
RCY	Radiochemical yield
MeCN	Acetonitrile
TEA	Triethylamine
GMP	Good manufacturing process
cGMP	Current good manufacturing process

Acknowledgements

This work was supported by the Cancer Research UK – Cancer Imaging Centre (C1060/A16464) and NIHR Clinical Research Facility at the Royal Marsden and ICR.

References

- 1 S. Vallabhajosula, *Semin. Nucl. Med.*, 2007, 37, 400–419.
- 2 P. W. Miller, N. J. Long, R. Vilar and A. D. Gee, *Angew. Chem., Int. Ed.*, 2008, 47, 8998–9033.
- 3 O. Jacobson, D. O. Kiesewetter and X. Chen, *Bioconjugate Chem.*, 2015, 26, 1–18.
- 4 J.-L. Zeng, J. Wang and J.-A. Ma, *Bioconjugate Chem.*, 2015, 26, 1000–1003.
- 5 C. Da Pieve, L. Allott, C. D. Martins, A. Vardon, D. M. Ciobota, G. Kramer-Marek and G. Smith, *Bioconjugate Chem.*, 2016, 27, 1839–1849.
- 6 P. Laverman, W. J. McBride, R. M. Sharkey, D. M. Goldenberg and O. C. Boerman, *J. Labelled Compd. Radiopharm.*, 2014, 57, 219–223.



- 7 W. J. McBride, C. A. D'Souza, H. Karacay, R. M. Sharkey and D. M. Goldenberg, *Bioconjugate Chem.*, 2012, **23**, 538–547.
- 8 J. P. Meyer, J. L. Houghton, P. Kozlowski, D. Abdel-Atti, T. Reiner, N. V. Pillarsetty, W. W. Scholz, B. M. Zeglis and J. S. Lewis, *Bioconjugate Chem.*, 2016, **27**, 298–301.
- 9 G. Niu, L. Lang, D. O. Kiesewetter, Y. Ma, Z. Sun, N. Guo, J. Guo, C. Wu and X. Chen, *J. Nucl. Med.*, 2014, **55**, 1150–1156.
- 10 Z. Varasteh, O. Åberg, I. Velikyan, G. Lindeberg, J. Sørensen, M. Larhed, G. Antoni, M. Sandström, V. Tolmachev and A. Orlova, *PLoS One*, 2013, **8**, e81932.
- 11 S. Boschi, J. T. Lee, S. Beykan, R. Slavik, L. Wei, C. Spick, U. Eberlein, A. K. Buck, F. Lodi, G. Cicoria, J. Czernin, M. Lassmann, S. Fanti and K. Herrmann, *Eur. J. Nucl. Med. Mol. Imaging*, 2016, **43**, 2122–2130.
- 12 W. J. McBride, C. A. D'Souza, R. M. Sharkey and D. M. Goldenberg, *Appl. Radiat. Isot.*, 2012, **70**, 200–204.
- 13 C. Yu, D. Pan, B. Mi, Y. Xu, L. Lang, G. Niu, M. Yang, W. Wan and X. Chen, *Eur. J. Nucl. Med. Mol. Imaging*, 2015, **42**, 2021–2028.
- 14 P. Laverman, W. J. McBride, R. M. Sharkey, A. Eek, L. Joosten, W. J. Oyen, D. M. Goldenberg and O. C. Boerman, *J. Nucl. Med.*, 2010, **51**, 454–461.
- 15 P. Laverman, C. A. D'Souza, A. Eek, W. J. McBride, R. M. Sharkey, W. J. Oyen, D. M. Goldenberg and O. C. Boerman, *Tumour Biol.*, 2012, **33**, 427–434.
- 16 J. Guo, L. Lang, S. Hu, N. Guo, L. Zhu, Z. Sun, Y. Ma, D. O. Kiesewetter, G. Niu, Q. Xie and X. Chen, *Mol. Imaging Biol.*, 2014, **16**, 274–283.
- 17 D. Shetty, S. Y. Choi, J. M. Jeong, J. Y. Lee, L. Hoigebazar, Y.-S. Lee, D. S. Lee, J.-K. Chung, M. C. Lee and Y. K. Chung, *Chem. Comm.*, 2011, **47**, 9732–9734.
- 18 J. Yang, M. R. Karver, W. Li, S. Sahu and N. K. Devaraj, *Angew. Chem., Int. Ed.*, 2012, **51**, 5222–5225.
- 19 D. Ory, J. Van den Brande, T. de Groot, K. Serdons, M. Bex, L. Declercq, F. Cleeren, M. Ooms, K. Van Laere, A. Verbruggen and G. Bormans, *J. Pharm. Biomed. Anal.*, 2015, **111**, 209–214.
- 20 C. Pascali, A. Bogni, L. Fugazza, C. Cucchi, O. Crispu, L. Laera, R. Iwata, G. Maiocchi, F. Crippa and E. Bombardieri, *Nucl. Med. Biol.*, 2012, **39**, 540–550.
- 21 K. Hayashi, K. Furutsuka, M. Takei, M. Muto, R. Nakao, H. Aki, K. Suzuki and T. Fukumura, *Appl. Radiat. Isot.*, 2011, **69**, 1007–1013.
- 22 G. Reischl, W. Ehrlichmann, C. Bieg, C. Solbach, P. Kumar, L. I. Wiebe and H. J. Machulla, *Appl. Radiat. Isot.*, 2005, **62**, 897–901.
- 23 R. Fortt, G. Smith, R. O. Awais, S. K. Luthra and E. O. Aboagye, *Nucl. Med. Biol.*, 2012, **39**, 1000–1005.
- 24 D. R. Turton, H. M. Betts, D. Dutton and A. C. Perkins, *Nucl. Med. Biol.*, 2015, **42**, 494–498.
- 25 A. F. Brooks, J. J. Topczewski, N. Ichiishi, M. S. Sanford and P. J. Scott, *Chem. Sci.*, 2014, **5**, 4545–4553.

